Optics and Laser Technology xxx (2017) xxx–xxx

Contents lists available at ScienceDirect

Optics and Laser Technology

journal homepage: www.elsevier.com/locate/optlastec

Full length article

Broadband photoluminescence of silicon nanowires excited by near-infrared continuous wave lasers

Zongbao Li [b,c], Xin Wang [c], Shaojing Liu [c], Jianxin Yang [c], KeZhang Shi [c], Haiyan Wang [d], Debin Zhu [a], Xiaobo Xing [a,c,*]

[a] MOE Key Laboratory of Laser Life Science & Institute of Laser Life Science, College of Biophotonics, South China Normal University, Guangzhou 510631, China
[b] School of Material and Chemical Engineering, Tongren University, Guizhou 554300, China
[c] South China Academy of Advanced Optoelectronics, South China Normal University, Guangzhou 510006, China
[d] School of Information Technology, Guangdong Industry Polytechnic, Guangzhou 510330, China

ARTICLE INFO

Article history:
Received 1 August 2017
Accepted 19 September 2017
Available online xxxx

Keywords:
Silicon nanowires
Photoluminescence (PL)
Upconversion
Near-infrared laser

ABSTRACT

In advanced nanomaterials field, silicon nanowires (SiNWs) play an increasing significant role due to the outstanding optical properties. Although various kinds of investigations for SiNWs in optical characteristic have been proposed, it remained rare study of the photoluminescence (PL) phenomenon. Here, we theoretically and experimentally demonstrate an upconversion PL with broadband spectrum by exciting SiNWs using 980 nm continuous wave laser. PL spectra are efficiently detected and range from 500 nm to 920 nm. An electron can be transferred to higher excitation energy levels by absorbing one photon with the assistance of multi-phonons, producing hot luminescence. The proposed concept of PL phenomenon can be extended to biosensor, fluorescence labeling systems, and miniature broadband optical source emitters.

1. Introduction

Silicon nanowires (SiNWs) have attracted enormous attention due to their potential applications in optical [1], nanoelectronic [2] and thermoelectric fields [3]. For now, the investigation of SiNWs not only contribute to the availably nanostructures [4] and optical properties [5–7], but also the significantly strong room-temperature photoluminescence (PL) and quantum size effects. Actually, based on the great potentials in SiNWs thin-film solar cells, the PL phenomenon and mechanisms of SiNWs have aroused extensive attentions. Initially, an unstable bright red PL was first observed for porous Si [8] and shifted into the visible for crystallite sizes below 5 nm while the quantum size effects theory was probably proposed to account for the mechanisms [9]. Because of the indirect band gap of Si, the weak light absorption and radiation in the visible light range have interdicted the further applications in photonics and so on [10]. Bandiera et al. [6] demonstrated that, with the periodic structures properly designed, the nanostructured Si could enhance the light absorption. The experimental result exposed that the crystalline-amorphous core-shell silicon nanowires exhibited extremely high absorption of 95% at short wavelengths ($\lambda < 550$ nm) and a concomitant very low absorption down to less than 2% at long wavelengths ($\lambda > 780$ nm) [7]. Excited by 337 nm and 488 nm laser light, Sivakov et al. reported a strong visible red-orange PL of rough silicon nanowire sidewalls at room temperature [4]. Ledoux et al. explored the mechanisms of PL based on different-size-SiNWs and presented a theoretically model to describe the quantum confinement of size to the PL for SiNWs [11]. Jing et al. also studied the effects of geometry on the mechanical properties of SiNWs and found that the fracture stress decreased as the periodic length increased [12]. These useful findings can provide insights into SiNWs fabrication and development of their applications.

Very recently, the results proved that, through hot-electron-assisted photocatalysis, the plasmonic nanoparticles could enhance the significant promise for solar energy [13]. Interestingly, the hot-electron-assisted catalysis efficiency was correlated with the intensity of the photoluminescence (PL) of gold nanoparticles and silver films [14]. It was found that such hot spots could emitted efficiently both up- and down-converted hot luminescence under excitation of femtosecond laser pulses. Different with the

* Corresponding author at: MOE Key Laboratory of Laser Life Science & Institute of Laser Life Science, College of Biophotonics, South China Normal University, Guangzhou 510631, China.
E-mail address: xingxiaobo@scnu.edu.cn (X. Xing).

https://doi.org/10.1016/j.optlastec.2017.09.031
0030-3992/

other upconversion physical mechanisms, the luminescence from such hot spots originated from the black-body emission of hot electrons generated by intraband transitions [15]. For SiNWs, the hot luminescence was confirmed to originate from the intraband transitions of electrons by using excitation photon energy smaller than its band-gap energy. To the best of our knowledge, the upconversion emission of SiNWs excited by the near-infrared light has not been investigated.

In this work, we have presented a broadband three-peaks-structure upconversion PL spectra of SiNWs excited by 980 nm continuous wave (CW) lasers. The upconversion physical mechanisms were also proposed to account for the main feature of the experimental phenomenon. The morphological characteristics of SiNWs were highly performed utilizing the SEM and Raman spectrometer. The spectra characteristic demonstrated that SiNWs could be rationally designed as light source emitters, which has significantly potential application for broadband optical source, biosensor, fluorescent labeling systems and so on.

2. Experimental details and discussions

The SiNWs were synthesized by metal-catalyzed electroless etching (MCEE) [16]. The detail fabrication was elaborated as follow: the n-Si (100) wafer pieces were cleaned by ultrasonically rinsing in acetone for 5 min and followed by acetone rinse for another 5 min. After the Si wafer pieces were boiled in H_2SO_4: H_2O_2 (3:1) for 30 min, they were guaranteed to be cleaned by rinsing with adequate deionized water (DW). The aqueous solution, 0.02 moles of silver nitrate ($AgNO_3$) and 5 moles of hydrofluoric acid (HF) in the volume ratio 1:1 solution, in sealed container was utilized to steep the cleaned Si wafer. The SiNWs were produced vertically after 30–60 min. Another copy of H_2SO_4-H_2O_2 solution was contributed to eliminate the silver dendritic on SiNWs surface. Finally, the surfaces obtained after the etching procedures were rinsed several times in DW and dried at room temperature. Structures analysis of SiNWs has been carried out by a JSM-7001F scanning electron microscope (SEM). Fig. 1a and b showed the as-prepared SiNWs array with the uniform length of ~6 μm and diameter in the range of 30–100 nm. The front view of SiNWs presented that our fabricated samples distributed uniformly in large area and cluster partly in small region. Fig. 1c gives out the UV–visible absorption spectra by using a PerkinElmer Lambda 950 UV–Vis-NIR spectrophotometer. From Fig. 1c, it can be seen that the absorption spectra of SiNWs are quite flat in the visible light range with a smooth peak appearing at about 400 nm. The results show that the SiNWs have high absorption efficiency in all visible regions. Scraped off from the silicon substrate in the alcohol solution, Fig. 2d exhibits the Raman spectra of the SiNWs samples under excitation of the CW laser with central wavelengths of 633 nm. The spectra shows remarkable Raman features at 519.9 cm^{-1}, which is good agreement with the theoretical calculations and experiments [17]. The Raman peak also shows a high purity SiNW samples without other impurities.

The PL experiments were carried out using a 980 nm laser for excitation at room temperature. Fig. 2 depicts the schematic illustration of the experiment. In order to eliminate the negative effect of the silicon substrate, the SiNWs were scraped off from the silicon substrate and mixed into absolute ethyl alcohol (EtOH). The finally SiNWs-EtOH suspension solutions with different concentration were obtained for PL. Then, an appropriate suspension was drawn onto a clean glass slide with a pipette. A CW laser light

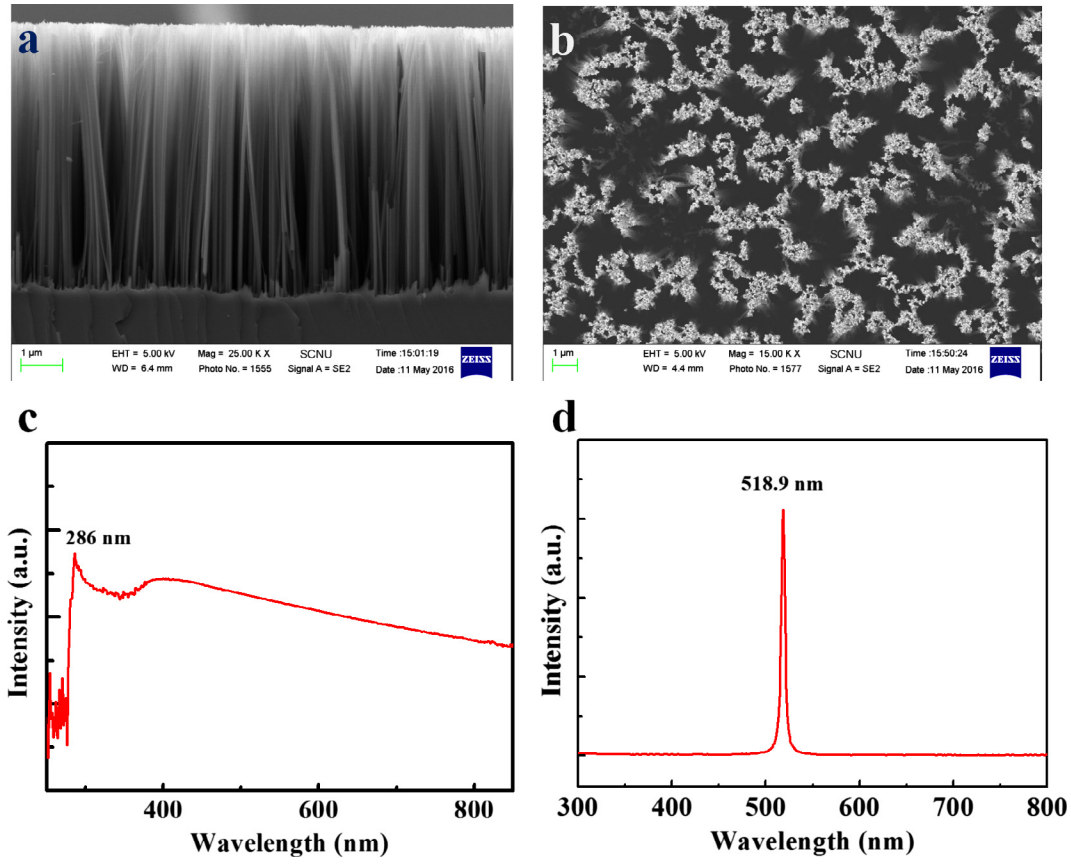

Fig. 1. Characteries of SiNWs. Typical SEM cross-section (a) and front-view (b) SEM images of SiNWs array after 5 cycles of DR process. (c) UV–vis spectra of SiNWs. (d) Raman spectra of SiNWs excited by 633 nm laser light source.

Please cite this article in press as: Z. Li et al., Broadband photoluminescence of silicon nanowires excited by near-infrared continuous wave lasers, Opt. Laser Technol. (2017), https://doi.org/10.1016/j.optlastec.2017.09.031

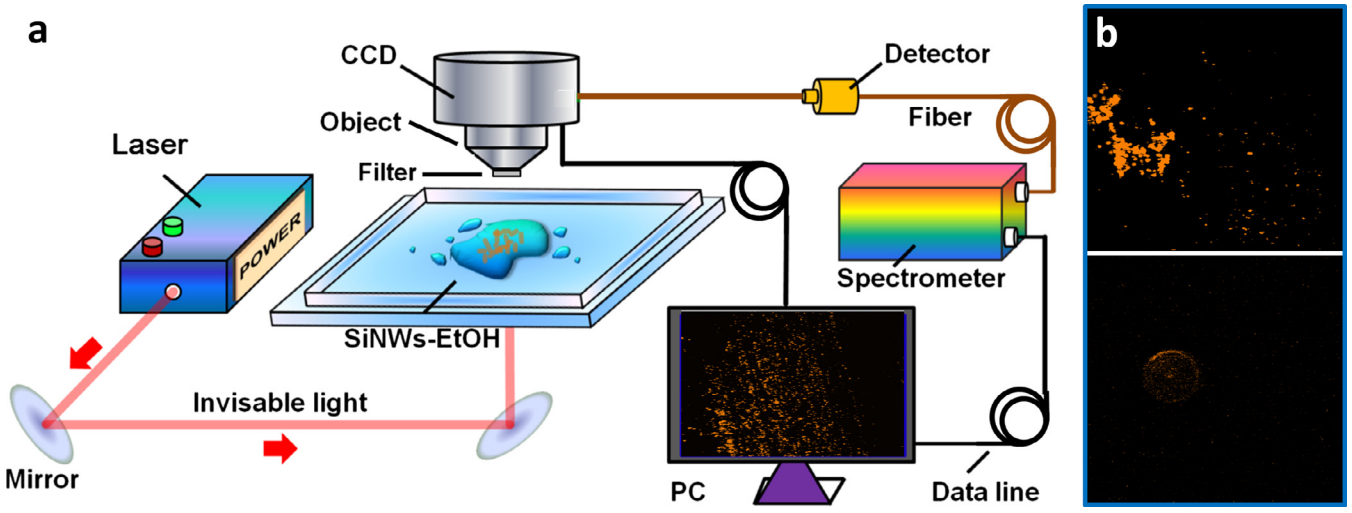

Fig. 2. Experimental schematic and characterization of photoluminescence of SiNWs. (a) Illustration of experimental setup. Red arrows indicated propagation of CW 980 nm light laser. A spectrometer with a 900 nm low-pass filter and fiber detector was utilized to collect the PL signals. (b) Overall view of PL image (up) and single one (down). (For interpretation of the references to color in this figure legend, the reader is referred to the web version of this article.)

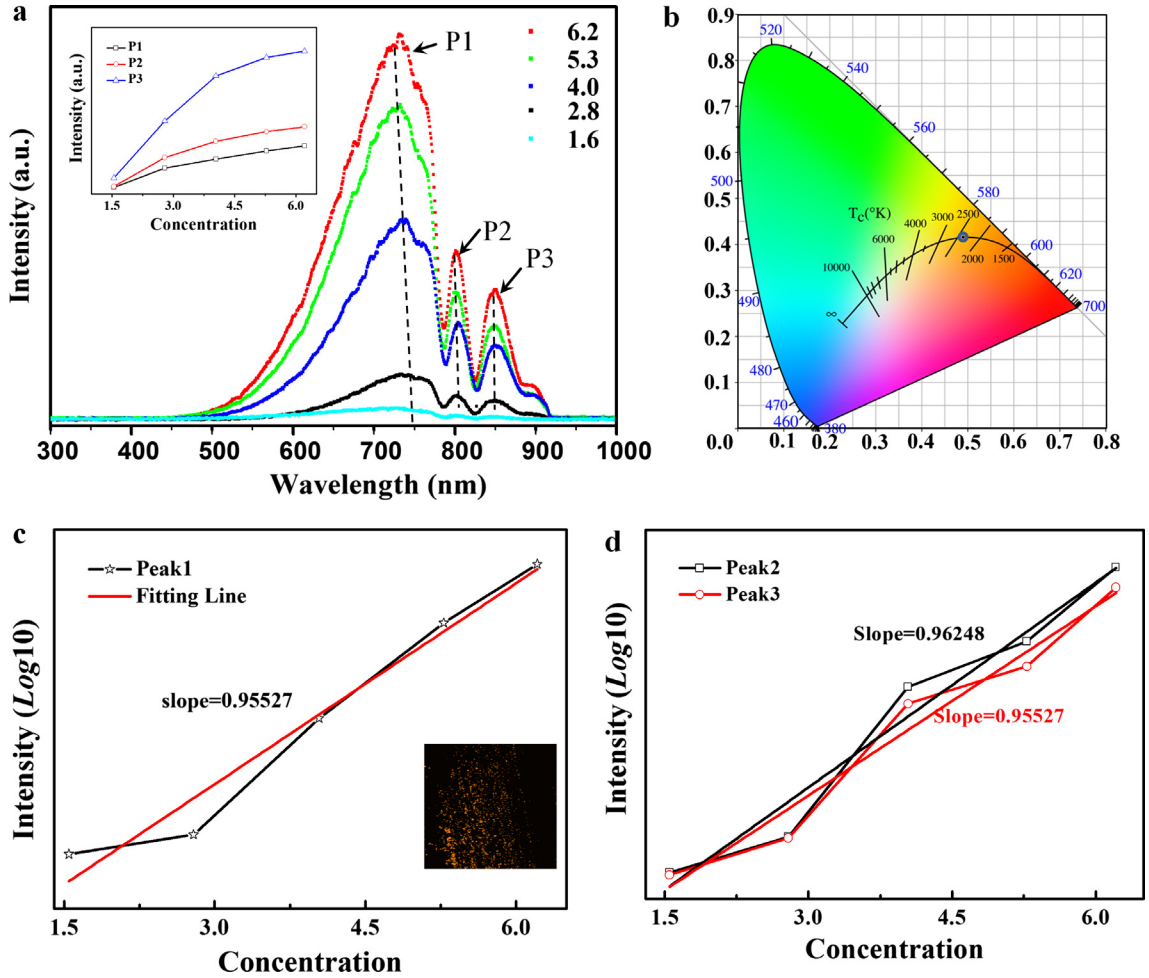

Fig. 3. (a) Hot luminescence spectra of SiNWs-EtOH suspension with different concentration. Inset is the FWHM intensity. (b) Chromaticity coordinates for whole upconversion emission. (c and d) Concentration dependence of upconversion luminescence intensity corresponding to the peak 1 (c), and peak 2 and peak 3 (d). Linear fit lines show the stable trend of the relationship.

(PS8147) with the center wavelength of 980 nm was used to illuminate the suspension solutions and an spectrometer (QE65000 Ocean Optics) with a 920 nm low-pass filter was used to collect the PL signals. Fig. 2b shows the bright orange luminescence image of the SiNWs in the dark field microscopy of the overall view and single one.

Please cite this article in press as: Z. Li et al., Broadband photoluminescence of silicon nanowires excited by near-infrared continuous wave lasers, Opt. Laser Technol. (2017), https://doi.org/10.1016/j.optlastec.2017.09.031

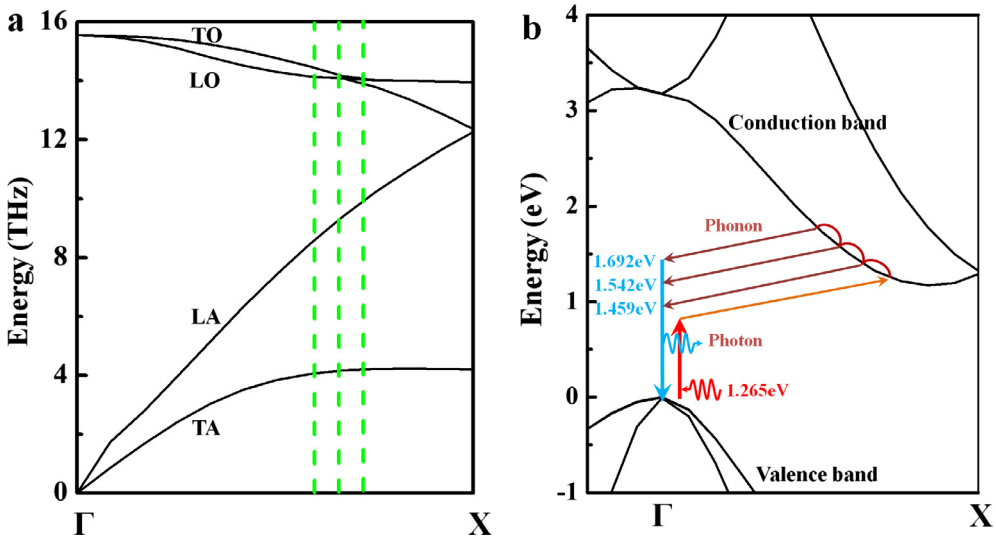

Fig. 4. Phonon dispersion and schematic band structure of crystalline silicon. (a) Phonon dispersion along dashed lines showing the phonon modes with high density of states at three different momentum values. (b) Electronic dispersion showing the corresponding energies at the same momentum values as high density phonons in (a), which explain the observed strong hot luminescence bands. The schematically possible hot luminescence processes with a photon and multi-phonons absorption in energy level diagrams were also given out.

Under 980 nm infrared CW laser excitation at 200 mW, Fig. 3a presents a broadband PL spectra ranging from 500 nm to 920 nm, for high counts obtained from various mass concentrations of SiNWs-EtOH suspensions as 6.2, 5.3, 4.0, 2.8 and 1.6 μg/ml. The observations suggest that the hot carriers emit photons through a phonon-assisted recombination process during intraband relaxation. As shown in the PL spectra, there are three peaks structure with the central wavelengths at about 733 nm (P1), 804 nm (P2), and 850 nm (P3). The similar spectra could also be observed for different mass concentrations. With the decrease of concentrations, the peaks show significant red shifts and flatten. The appearance of a gentle slope aside P1 indicates a phonon-assisted process while the decreasing gradual peak values are due to the proper momentum conservation law in three states. In addition, the exhibited relationships between the concentrations of SiNWs and full width at half maximum (FWHM) luminescence intensity of PL were given out in the inset. The results could be seen that the relationship exhibits logarithmic growth with concentration increases. From the CIE chromaticity in Fig. 3b, it could be seen that luminescence colors of the spectra appeared to be orange. The CIE also reveals that the temperature should reach about 2500 K if the orange emission was obtained only by blackbody radiation. Furthermore, to test the generality of visible hot luminescence in SiNWs, for each peaks, we can plot the luminescence intensity as a function of the concentration in a double logarithmic coordinate which generally show a straight line, as shown in Fig. 3c and d, while the slopes as 0.95527, 0.96248 and 0.95527 for peak 1 to peak 3. With the concentration increases gradually, the same slope values confirm that the emission photon numbers are positive proportional to the concentrations with the same absorption efficiency. Based on the finding, the results indicate that the phonon-assisted hot luminescence is greatly enhanced when the hot carriers are assisted by phonons with the higher concentration.

The broad three-peaks-structure spectra of the hot luminescence originated from a large number of discrete photon assisted with many pathways interacted with the phonons on each crystallographic direction of the electronic dispersion of SiNWs [18]. Due to the energy and momentum conservations, the existence of specific phonon modes provides highly emissive pathways for the phonon assisted hot luminescence process, resulting in the observed three strong emission peaks. It should be noted that the PL emission was only possible when the phonons scattered the hot carriers to the almost vertical light line. Based on the momentum conservation, the phonon-assisted scattering process should satisfy as $k' = k_e \pm n \cdot q \approx 0$, where k' and k_e are the momentum values of carriers at the light line and at the initial electronic state and q is the phonon momentum while n is the number of the participated phonons in the process. In SiNWs, the phonon dispersion along the ⟨1 0 1⟩ direction shows that the density of states is relatively high for momentum values situated between Γ and X points, as shown in Fig. 4a. Based on the results shown in Fig. 4b, the absorption process upon laser excitation (980 nm, 1.265 eV) involves interaction with multi-phonons to the higher energy points. Followed by intraband relaxation of hot carriers, the high-energy electron transitions will occur with luminescence and phonon emission. In the process, it occurs by a one-photon process involving an optical phonon near the Brillouin zone center (Γ-point) with low k-values [19]. Near the zone boundary, because of the much higher density of states of transverse acoustic (TA) phonons than that of longitudinal acoustic (LA) phonons in SiNWs, as shown in Fig. 4a, the above intraband relaxation process would be dominated by multi-TA phonons [20].

3. Conclusion

We have fabricated SiNWs on the silicon substrate by MCEE method and the characterized are discussed. The phonon-assisted hot luminescence of SiNWs with a three-peak structure has been demonstrated. Our results showed a linear-relationship between the mass concentration and luminescence intensity. Finally, a consequent of the broadband spectra in visible-region, was excited by the CW laser in near-infrared, the low-cost SiNWs were expected to be useful for the fabrication of monolithic devices utilizing optics for ultrafast data processing.

Acknowledgements

This work is partially supported by Guangdong Provincial Key Laboratory of Optical Information Materials and Technology (Grant No. 2017B030301007), Guangdong Natural Science Foundation

(2013B090500123, 2014A030313432, 2016A020221030, 2013B090500034), Guangdong Innovative Research Team Program (No. 2013C102) and Guangdong Province Grant (No. 2016B090909001), Pearl River S&T Nova Program of Guangzhou (201506040045), Guizhou Natural Science Foundation ([2016] 1150, 2017-(2014)-009), and National Natural Science Foundation of China (Nos. 61177077, 81371877). The authors thanks Sailing He for the help at the mechanism the phenomenon.

References

[1] L. Hu, G. Chen, Analysis of optical absorption in silicon nanowire arrays for photovoltaic applications, Nano Lett. 7 (2013) 3249–3252.
[2] Y. Cui, Z.H. Zhong, D.L. Wang, W.U. Wang, C.M. Lieber, High performance silicon nanowire field effect transistors, Nano Lett. 3 (2003) 149–152.
[3] A.I. Hochbaum, R.K. Chen, R.D. Delgado, W.J. Liang, E.C. Garnett, M. Najarian, A. Majumdar, P.D. Yang, Enhanced thermoelectric performance of rough silicon nanowires, Nature 451 (2008) 163–168.
[4] V.A. Sivakov, F. Voigt, A. Berger, G. Bauer, S.H. Christiansen, Roughness of silicon nanowire sidewalls and room temperature photoluminescence, Phys. Rev. B 82 (2010) 125446.
[5] B.H. Zhang, H.S. Wang, L.H. Lu, K.L. Ai, G. Zhang, X.L. Cheng, Large-area silver-coated silicon nanowire arrays for molecular sensing using surface-enhanced Raman spectroscopy, Adv. Funct. Mater. 18 (2008) 2348–2355.
[6] S. Bandiera, D. Jacob, T. Muller, F. Marquier, M. Laroche, J.J. Greffet, Enhanced absorption by nanostructured silicon, Appl. Phys. Lett. 93 (2008) 607.
[7] M.M. Adachi, M.P. Anantram, K.S. Karim, Optical properties of crystalline-amorphous core-shell silicon nanowires, Nano Lett. 10 (2010) 4093–4098.
[8] H.J. Lee, Y.H. Seo, D.H. Oh, K.S. Nahm, Y.B. Hahn, I.C. Jeon, E.K. Suh, Y.H. Lee, Light emission phenomena from porous silicon: siloxene compounds and quantum size effect, Appl. Phys. 75 (1994) 8060–8065.
[9] C.G. John, V.A. Singh, Theory of the photoluminescence spectra of porous silicon, Phys. Rev. B. 50 (1994) 5329–5334.
[10] G.G. Macfarlane, T.P. McLean, J.E. Quarrington, V. Roberts, Exciton and phonon effects in the absorption spectra of germanium and silicon, J. Phys. Chem. Solids 8 (1959) 388–392.
[11] G. Ledoux, O. Guillois, D. Porterat, C. Reynaud, F. Huisken, B. Kohn, V. Paillard, Photoluminescence properties of silicon nanocrystals as a function of their size, Phys. Rev. B 62 (2000) 15942–15951.
[12] Y. Jing, C. Zhang, Y. Liu, L. Guo, Q. Meng, Mechanical properties of kinked silicon nanowires, Physica B. 462 (2015) 59–63.
[13] S. Linic, P. Christopher, D.B. Ingram, Plasmonic-metal nanostructures for efficient conversion of solar to chemical energy, Nat. Mater. 10 (2011) 911–921.
[14] T. Haug, P. Klemm, S. Bange, J.M. Lupton, Hot-electron intraband luminescence from single hot spots in noble-metal nanoparticle films, Phys. Rev. Lett. 115 (2015) 067403.
[15] Y. Zheng, H. Liu, J. Xiang, Q. Dai, M. Ouyang, S. Tie, Hot luminescence from gold nanoflowers and its application in high-density optical data storage, Opt. Express 25 (2017) 9262.
[16] X. Wang, K.Q. Peng, X.J. Pan, X. Chen, Y. Yang, L. Li, X.M. Meng, W.J. Zhang, S.T. Lee, High-performance silicon nanowire array photoelectrochemical solar cells through surface passivation and modification, Angew. Chem. Int. Ed. 50 (2011) 9861–9865.
[17] B.B. Li, D.P. Yu, S.L. Zhang, Raman spectral study of silicon nanowires, Phys. Rev. B 59 (1999) 1645–1648.
[18] C.H. Cho, C.O. Aspetti, J. Park, R. Agarwal, Silicon coupled with plasmon nanocavity generates bright visible hot-luminescence, Nat. Photonics 7 (2013) 285.
[19] W. Racek, G. Bauer, H. Kahlert, Dynamic measurement of hot-electron magnetophonon effect in n-InSb at 11 K, Phys. Rev. Lett. 31 (1973) 301–304.
[20] S. Wei, M.Y. Chou, Phonon dispersion of silicon and germanium from first-principles calculations, Phys. Rev. B 50 (1994) 2221–2226.

Please cite this article in press as: Z. Li et al., Broadband photoluminescence of silicon nanowires excited by near-infrared continuous wave lasers, Opt. Laser Technol. (2017), https://doi.org/10.1016/j.optlastec.2017.09.031